Agricultural Water Management 208 (2018) 43–58

Contents lists available at ScienceDirect

Agricultural Water Management

journal homepage: www.elsevier.com/locate/agwat

Shallow groundwater plays an important role in enhancing irrigation water productivity in an arid area: The perspective from a regional agricultural hydrology simulation

Xiaoyu Gao[a,b], Zailin Huo[a,*], Xu Xu[a], Zhongyi Qu[b,**], Guanhua Huang[a], Pengcheng Tang[c], Yining Bai[d]

[a] Centre for Agricultural Water Research in China, China Agricultural University, Beijing, 100083, China
[b] Water Conservancy and Civil Engineering College, Inner Mongolia Agricultural University, Hohhot, 010018, China
[c] Institute of Water Resources for Pastoral Area, China Institute of Water Resources and Hydropower Research, Hohhot, 010020, China
[d] Water Resources Research Institute, New Mexico State University, Las Cruces, 88001, United States

ARTICLE INFO

Keywords:
Irrigation area
Shallow groundwater
Agricultural hydrology modeling
Agricultural water productivity

ABSTRACT

Agricultural water productivity (WP) is an important indicator to evaluate the implementation of agricultural water saving in arid regions. However, the role of groundwater capillary rise to crop water use and WP is unclear at the regional scale, as the soil texture, irrigation amount, planting pattern and groundwater depth is various for different fields. Based on the calibrated Agricultural Water Productivity Management for Shallow Groundwater (AWPM-SG) model, a five-year regional WP and water budgets assessment was performed. The results showed that the groundwater contribution to crop evapotranspiration (ET) would be up to 65% with a groundwater depth of 1.0–1.5 m, but the agricultural productivity would be relatively low resulting from a waterlogged root zone. Additionally, deep groundwater could result in a reduced WP due to less capillary rise, while WP would be 2.02 and 1.98 kg/m^3 with groundwater depth of 2.5–3.0 m and 3.0–4.5 m under irrigation amount of 100–300 mm. Furthermore, limited irrigation can enhance the contribution of groundwater to WP and irrigation water productivity (IWP), which is significant with groundwater depth increasing. While the average IWP were 5.83, 3.62, 2.54 and 1.77 kg/m^3, respectively for irrigation amount of 100–300, 300–500, 500–700 and 700–900 mm and the average IWP decreased from 4.79 m to 3.18 kg/m^3 with groundwater depth increasing 0.5–1.0 m to 3.0–4.5 m. However, irrigation effective utilization (C_{ieu}) was affected by groundwater depth weakly with irrigation water increasing. Furthermore, the optimal groundwater depth of 2.5–3.0 m was obtained by the impact of groundwater on irrigation water productivity (IWP) and C_{ieu}. Thus at the regional scale, the spatial distribution of groundwater levels needs to be considered for making irrigation decisions.

1. Introduction

Water scarcity has become a serious limiting factor for worldwide agricultural and economic development with increasing food demands and populations. However, compared with developed countries, water productivity is low in most developing countries. In many semi-arid and arid regions of the world, irrigated agriculture accounts for 90% of the total water use. Improving agricultural water productivity is a priority for ensuring water and food security (Dalin et al., 2015). Therefore, improving irrigation efficiency is becoming more important to increase agricultural water productivity.

Agricultural water saving directly changes the soil water content of the root zone and groundwater upward flux, which causes changes to the agricultural water cycle and crop growth (Bouman, 2007; Morison et al., 2008; Jaksa and Sridhar, 2015). Agricultural water cycles are the driving processes for agricultural water productivity, and the complex relationships between crop water consumption, soil water content, groundwater and irrigation at the regional scale are still unclear. Therefore, based on understanding the linked process of crop growth and agricultural water cycles, quantifying the effect of agricultural water saving on agricultural water productivity is the basis for realizing effective water use.

Especially in a shallow groundwater district, like the Hetao irrigation district, groundwater levels apparently fluctuate as a result of

* Corresponding author at: No. 17, Qinghua East Road, Haidian, Beijing, China.
** Corresponding author at: No. 306, Zhaowuda Road, Saihan, Hohhot, China.
E-mail addresses: huozl@cau.edu.cn (Z. Huo), quzhongyi@imau.edu.cn (Z. Qu).

https://doi.org/10.1016/j.agwat.2018.06.009
Received 22 September 2017; Received in revised form 27 May 2018; Accepted 7 June 2018
Available online 14 June 2018

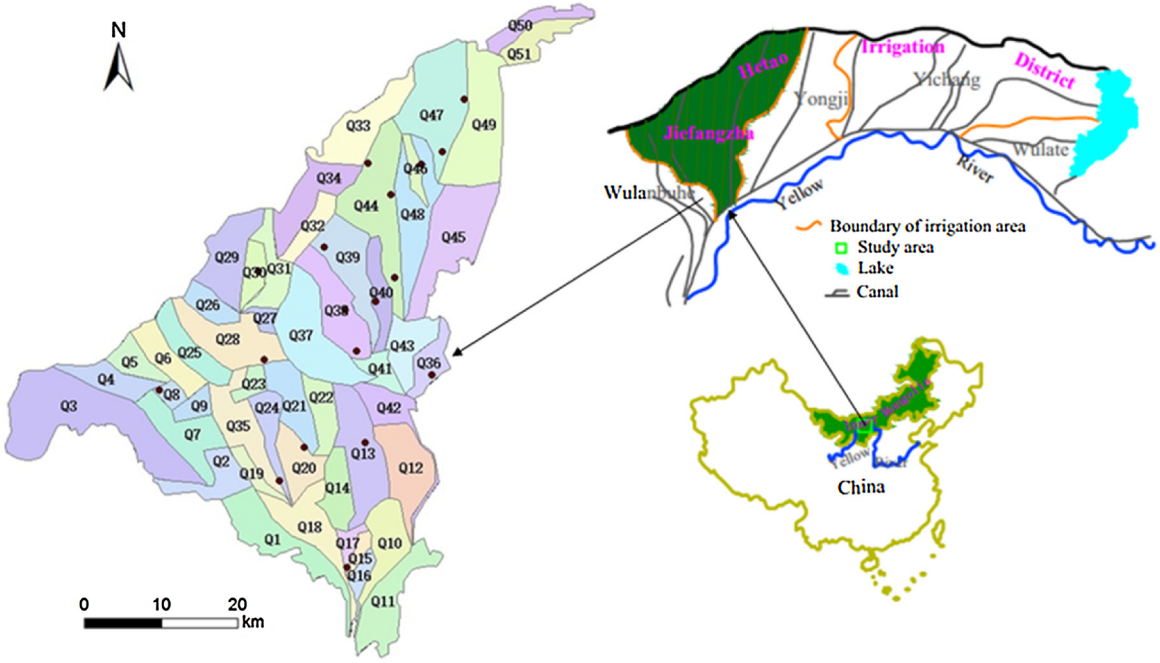

Fig. 1. Location of the study area and observation sites. The dots in the left figure are sites with measured data.

irrigation over the crop growing period (Xu et al., 2015) and the agricultural water cycle becomes more complex. With the implementation of water saving strategies, the exchange between soil water and groundwater will be changing with declining groundwater. Furthermore, the groundwater upward flux in the water table needs quantification due to its significance for crop water use (Yang et al., 2007; Huo et al., 2012).

The capillary rise from the water table is affected by several factors such as depth to groundwater, soil hydraulic properties, crop growing stage and irrigation amount. Many researchers have focused on the influencing factors of capillary rise (Santoni et al., 2010; Nishida and Shiozawa, 2010; Liu et al., 2016). Based on the irrigation field experiment and weighing lysimeters experiment, results showed that groundwater contributions amounted to approximately 40% of the total ET of maize with a groundwater depth of 0.5 m and groundwater contribution to crop water use of safflower for the treatments without supplementary irrigation under 0.6 m deep groundwater were 72% (Ragab and Fathi, 1986; Soppe and Ayars, 2003; Ghamarnia et al., 2013).

However, due to their inconvenience and expensive maintenance of field experimental methods, the process based models are preferred to quantify the capillary rise. The groundwater-soil-plant-atmosphere continuous (GSPAC) system is important to understand the agricultural water cycle (Wang et al., 2004; Zhou et al., 2005; Li et al.,2011). Numerical models such as HYDRUS (Simunek et al., 2005) and SWAP (Van Dam Jos et al., 2008) require many soil and crop parameters, which limit the use of models to some extent (Schoups et al., 2005). In contrast, conceptual models of agricultural water cycles based on the water balance method are widely used due to their simple structure and limited parameters. Considering the impact of soil water on the crop ET, some studies incorporated a root uptake model in the water balance model (Kendy et al., 2003).

Agricultural water productivity is not only related to the water cycle process but also to the crop growing process. In agricultural water management, the relationship between crop yield and crop ET is often characterized using a water production function based on abundant field experiments, but it ignores the formation process of crop growing, development final biomass and yield and ET. Therefore, crop models become important to quantify the agricultural WP. Models such as SUCROS (De Wit et al., 1970) and WOFOST (Diepen et al., 1989), reveal the crop growth process and the effect of environmental factors on crop growth. These models require many crop parameters which are not readily available. Alternatively, simpler versions for describing physiological and biochemical process are used widely, such as the DSSAT model (Jones et al., 2003) and EPIC model (Williams, 1995). Due to the great applicability, these models have been used for agricultural management at a regional scale (Cynthia et al., 2014).

The integration of crop and hydrological models is becoming more and more popular for evaluating agricultural WP. For example, the SWAP model linked to the WOFOST model (Van Dam Jos et al., 2008), the RZWQM model coupled the DSSAT model with soil dynamic process (Hanson et al., 1998), and the Aquacrop model coupled the simple crop model and concept model of soil water (Vanuytrecht et al., 2014). With the improvement of GIS and remote sensing, the distributed model has become an often used method for studying hydrological processes at the regional scale (Xue et al., 2017). Various examples confirm the appropriateness of GIS applications in groundwater hydrology (Herzog et al., 2003; Jha et al., 2007; Brunner et al., 2008).

Considering the above, the aim of this study is to prove contribution of groundwater capillary rise to ET at regional scale with various crops and soils. This is important to optimize the irrigation management and design the reasonable water-saving irrigation practices to improve irrigation water productivity by considering groundwater capillary rise to ET. With the calibration and application of agricultural WP management model (AWPM-SG) (Gao et al., 2017a,b) in the Jiefangzha Irrigation Area (JFZIA) of the Hetao irrigation district, the detailed objectives of this study are: (1) to indicate spatial and temporal distribution of groundwater upflow flux and effectivity of irrigation water in an irrigation district; (2) identify the dependence of groundwater capillary rise contribution to regional evapotranspiration (F/ET) on groundwater depths; (3) determine the impact of irrigation amounts and groundwater depth on water productivity.

2. Materials and methods

2.1. The study area and data

The Jiefangzha Irrigation Area (JFZIA), a typical irrigation area

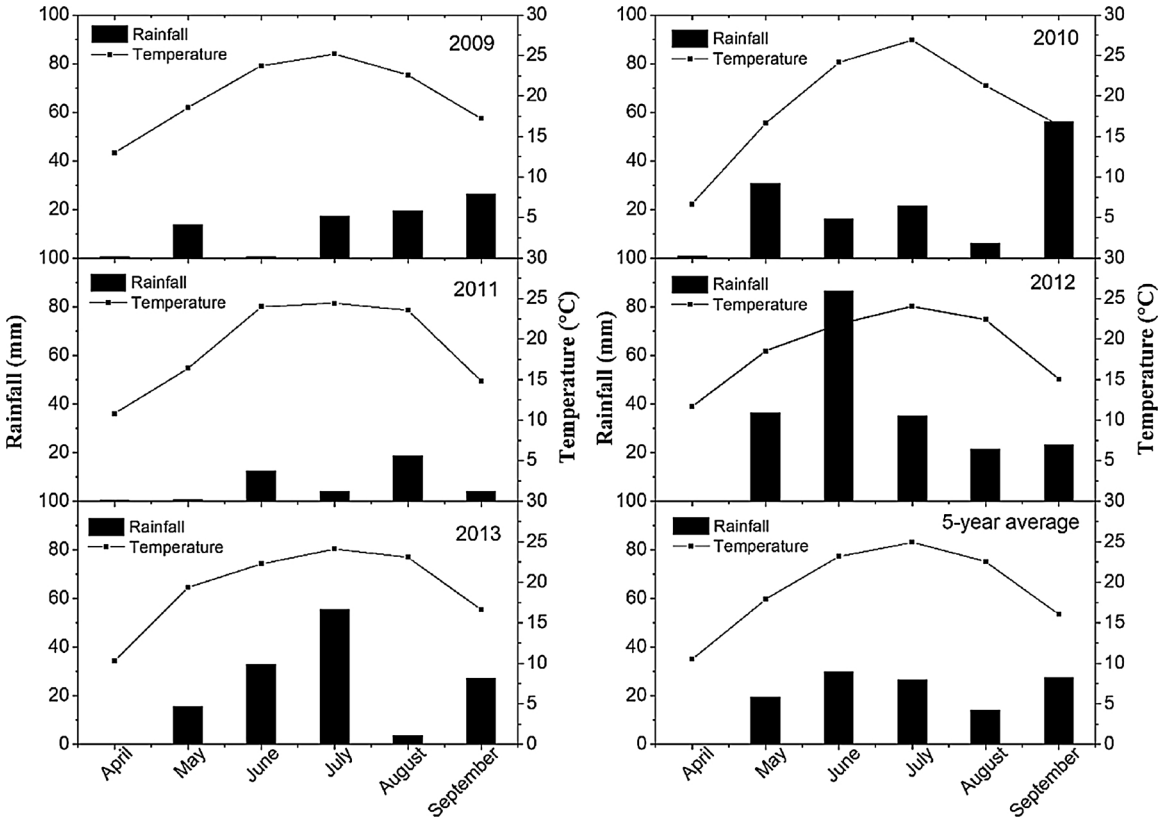

Fig. 2. Monthly rainfall and temperature in the Jiefangzha Irrigation area during 2009–2013.

with shallow groundwater, was chosen as the study area. With an area of 1.12 Mha, the JFZIA is a typical region of the Hetao irrigation district, which is located in the southeast of the Lang Mountains and northwest of the Yellow River, one of the largest irrigation districts in China (Fig. 1). The topography of this area descends from the southeast to northeast with an average slope of 0.02% (Xu et al., 2010).

The region has a typical arid and semi-arid continental climate. The region has high temperature and drought in summer along with cold and less snow in the winter. The monthly average temperature is −10.1 °C in January and 23.8 °C in July (Xu et al., 2010). The average monthly temperature from April to September ranged from 10.49 °C–24.93 °C during 2009–2013. Annual average pan evaporation is approximately 2000 mm, while precipitation is only 155 mm. In addition, 80% of the precipitation occurs from April to September. Irrigation is required in this area throughout the crop growing season. There are 3100–3300 hours of sunshine and 135–150 frost-free days per year. The average elevation of this study area is 1056 m. The meteorological data during 2009 to 2013 are shown in Fig. 2.

Soils in the study were spatially heterogeneous with primarily silt loam and silt in the northern region and silt loam and sandy loam in the southern region (Fig. 3). The soil begins to freeze in the middle of November and is frozen completely until late April or early May (Cai et al., 2003). In May, the soil begins to thaw and the groundwater depth decreases.

Wheat, maize and sunflower were the three main crops and account for 85% of total crop-land in the study area. Due to low quantities of rainfall, irrigation is necessary during the crop growing season. The primary irrigation method is flood irrigation, with an average application of 8000 m^3/ha for the crop growing season. It was observed that there was an autumn irrigation practice with an average application of 2600 m^3/ha after the harvest of crops each year. The aims of the autumn irrigation are to store up water in the soil for the next crop planting. The mean soil salinity in this region was relatively low, with 3.8 ms/cm less than the mean threshold for the three crops (Allen et al., 2006), and the effect of soil salinity on crop growth was ignored in this study.

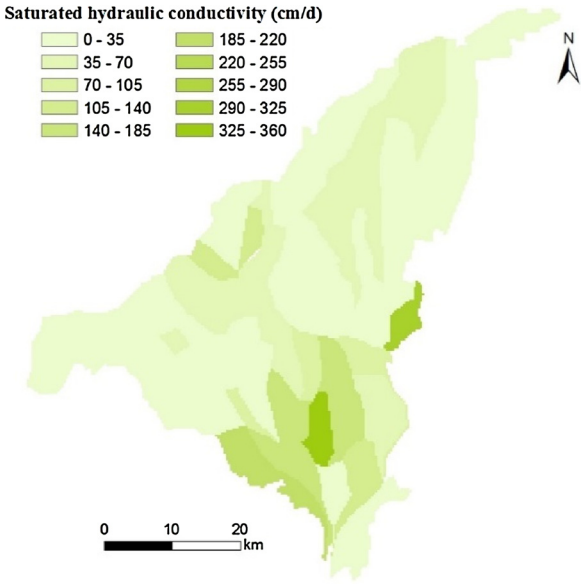

Fig. 3. Spatial distribution of soil saturated hydraulic conductivity in the Jiefangzha Irrigation Area during 2009–2013.

The Yellow River is the main water source of this irrigation district, with annual water supplication of approximately 47.89 × 10^8 m^3. The irrigation amount, irrigation time and irrigation area were obtained from the Hetao Irrigation Administration Bureau. In recent years, water-saving irrigation was widely applied in this region. The irrigation amount was various in different regions. A total of 51 irrigation units were determined by the corresponding control canals. The distributions

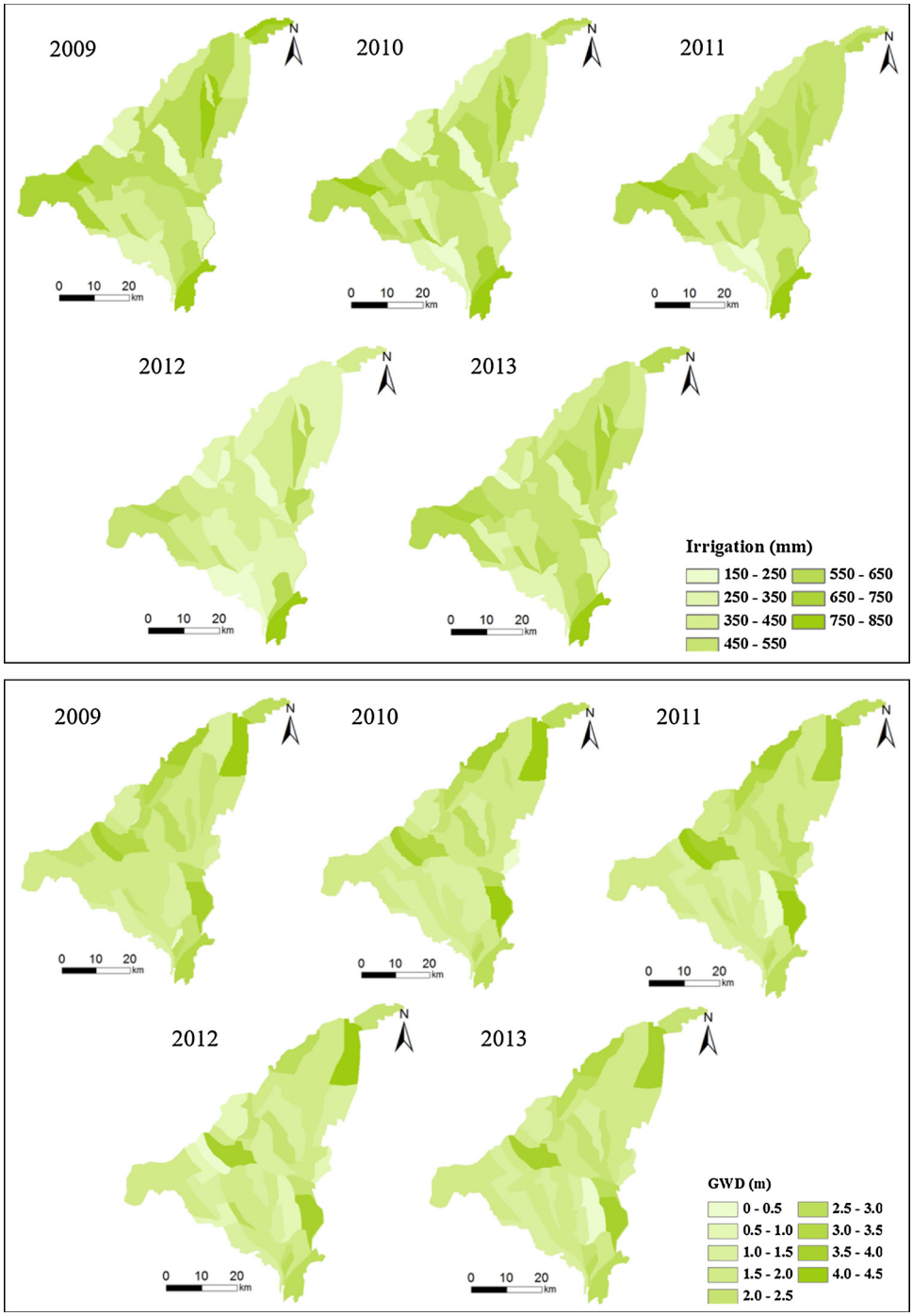

Fig. 4. Spatial distribution of irrigation amount and groundwater depth in the Jiefangzha Irrigation Area during 2009–2013. I is irrigation amount (mm). GWD is groundwater depth (m).

of the irrigation amount in the study area during 2009–2013 are shown in Fig. 4. According to the distribution of the main canals, the study area was divided into four main sections including Wulahe, Qinghui, Yangjiahe and Huangji. The majority of total irrigation was focused on Wulahe and northeast of Huangji. The average irrigation amount in 2012 was lower than that in 2013, which was due to more precipitation in 2012.

The groundwater depth at 51 sites was measured every five days from 2009 to 2013. During the five years, the groundwater depth of 51 sites ranged from 0.1 m to 5.57 m in the JFZIA. The spatial distributions of groundwater depth during 2009–2013 are shown in Fig. 4. In most of the region, the groundwater depth was shallower than 3.0 m. The average groundwater depth of the Wulahe, Yangjiahe, Huangji and Qinghui irrigation area during 2009–2013 were 1.50 m, 1.98 m, 2.09 m and 2.23 m, respectively. With the implementation of water-saving measurements, the average groundwater depth increased from 1.96 m in 2009 to 2.12 m in 2011. Then with more precipitation in 2012, the average groundwater depth became 1.78 m in 2012 and 1.92 m in 2013.

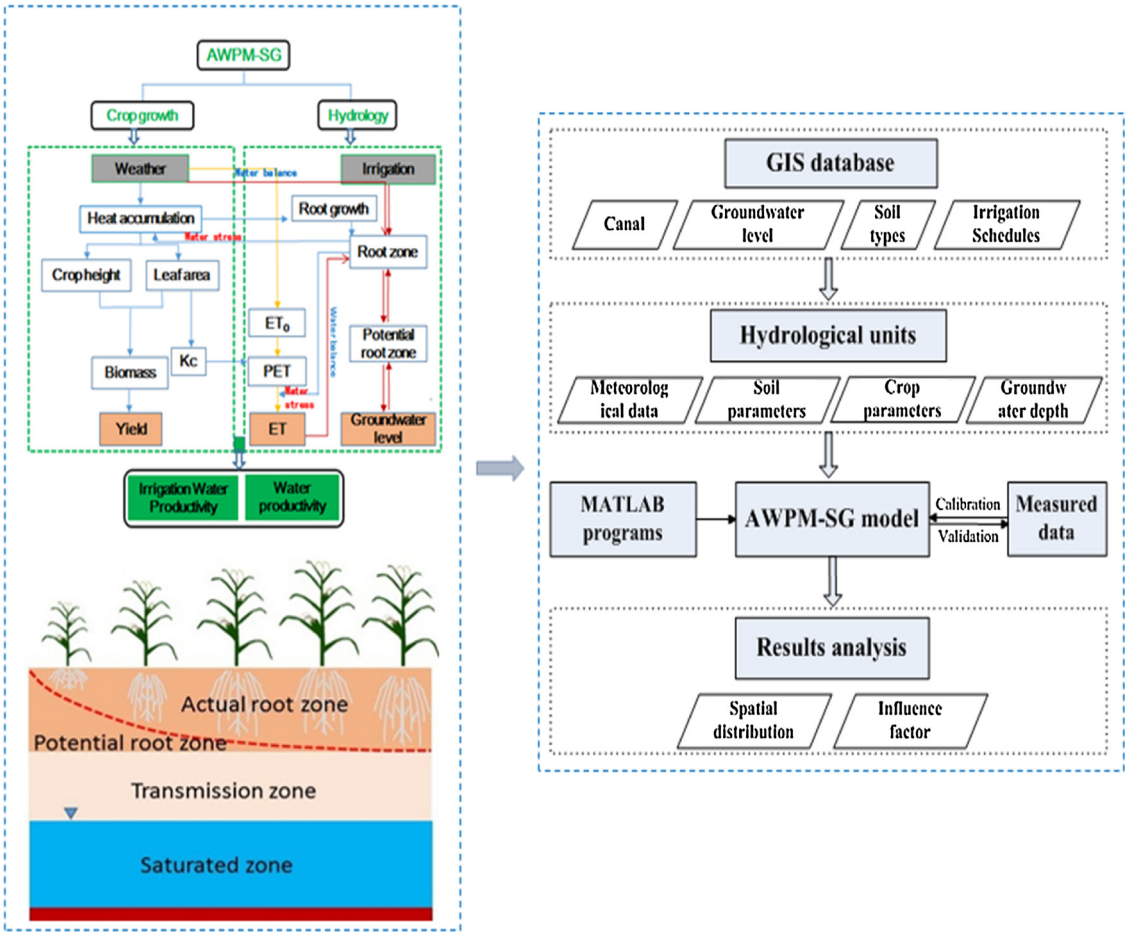

Fig. 5. The schematic of regional simulation using AWPM-SG model.

2.2. Regional agricultural water productivity simulation method

2.2.1. Agricultural water productivity with shallow groundwater model at field scale

In a previous study, the Agricultural Water Productivity Management with Shallow Groundwater (AWPM-SG) model was developed and validated at the field scale (Gao et al., 2017a,b). The model couples the soil water, groundwater and crop growth processes (Saleh et al., 1989; Williams, 1995). The AWPM-SG model consists of three parts: a crop module, an actual ET module and a soil module. An overview of the AWPM-SG model is given in Fig. 5. In this study, the AWPM-SG model was used to simulate the spatial distribution of water fluxes, crop ET, crop yield, water productivity and irrigation water productivity at the regional scale.

In the AWPM-SG model, the crop module is mainly based on the EPIC model (Environmental Policy Integrated Climate) developed by Williams et al. (Williams et al., 1989). Based on the temperature accumulation process, the crop module consists of phenological development, crop growth indicators (LAI, biomass, root development and crop yield), water productivity and irrigation water productivity (WP and IWP).

EPIC was coupled with the modified watershed irrigation potential estimation model (WIPE) to simulate the flux of the groundwater-soil water-crop water consumption system. The WIPE model was developed by Saleh et al. (1989) to study the impact of irrigation management schemes on groundwater levels in Bangladesh (Saleh et al., 1989). Precipitation, irrigation, soil properties such as moisture content and hydraulic conductivity, and the initial groundwater level are required to run this model. In this mode, the soil profile was divided into four zones: the actual root zone (zone 1), potential root zone (zone 2), transmission zone (zone 3), and the saturated zone (zone 4), which are shown in Fig. 5. Zone 1 is the zone occupied by roots; zone 2 is the zone that is not currently occupied by the roots but will be so after their complete development; zone 3 is the unsaturated transition zone below the root zone with a lower boundary at water table and the thickness of this layer varies in time according to extraction/evaporation and recharge; and zone 4 is the saturated zone and is regarded as the water table. Zone 3 is always at a constant moisture content and is equal to the saturated moisture content minus the drainable porosity. During the simulation process, the soil texture in zones 1 and 2 were the same. The water balance method was used for the water movement calculation of zone 1.

When $RD_i \leq RD_{mx}$, *water balance is calculated in the zone 1*

$$Wr_{i+1} = Wr_i + P + I + CAP + CR - ET - P_w \quad (1)$$

Where RD_i and RD_{mx} are current root depth and maximum root depth (mm); Wr is water content in the zone 1(mm); P is precipitation (mm), I is irrigation (mm), ET is actual evapotranspiration (mm); CR is the water depth supplied to the root zone from deeper zone due to the root growth (mm); P_w is the water depths that leave the current root zone (mm); CAP is the capillary rise from zone 2 (mm) (Ritchie, 1972).

Water balance calculation of zone 2:

When $mg \geq \theta_{fc}$ (field capacity) where θ_{fc} is the redistribution moisture content of root zone and the flux J is given by (Saleh et al., 1989)

$$J = d_2 * \{mg + \frac{\theta_s - \theta_r}{C} * \ln\left[\frac{C * k_2 s * \exp(-C)}{d_2 * (\theta_s - \theta_r)} + \exp\left(-C * \frac{mg - \theta_r}{ms - \theta_r}\right)\right] - \theta_r\} \quad (2)$$

Which is always directed downwards (mm). Here d_2 is the thickness of zone 2, which equals to maximum root depth minus current root depth (mm), *mg* are the soil moisture in the zone 2 (cm^3/cm^3), θ_s is the saturated moisture content of root zone (cm^3/cm^3), θ_r is the air-dry moisture content of root zone (cm^3/cm^3), k_2s is the saturated hydraulic conductivity of root zone (mm/day), which is measured in 100 cm^3 undisturbed soil samples of 51 sites in JFZIA using a constant-head permeameter (Wit, 1967), and *C* is a constant to 13. In this condition, there will be no upward evaporation flux from the aquifer so flux = -J.

When $mg < \theta_{fc}$ there will not be any downward flux so that J = 0. However, the upward evaporative flux from the aquifer will be non-zero and is a function of depth to water table from soil surface as given by Gardner (1958)

$$u = ks * \left(\frac{e^{-\alpha\varphi}-1}{1-e^{\alpha h}}\right) \quad (3)$$

Where *ks* is the saturated hydraulic conductivity of transmission zone (mm/day), which is measured similar to k_2s. *h* is the depth to the water table (mm), which is obtained using the measured groundwater data. αis the diffusivity coefficient which is the inverse of air entry φ_h, φ is soil water potential (mm).

When $RD_i > RD_{mx}$, there will be no zone 2, the calculation of zone 1 is similar to zone 2 when $RD_i \leq RD_{mx}$.

In this study, measured groundwater depths were used as input. The soil module was a one-dimensional model employing the Thornthwaite-Mather procedure to calculate the recharge below the root zone to the aquifer which is primarily applicable to shallow aquifers (Steenhuis and Van Der Molen, 1985).

The actual ET was calculated based on soil water content, crop leaf index and potential crop ET (ET_p). In this model, the potential ET was obtained by the reference ET (ET_0) multiplied by the crop coefficient (K_c), which is related to crop leaf area (Sau et al., 2004). The ratio of potential evaporation (E_p) to potential transpiration (T_p) depends upon the developmental stage of the leaf canopy, soil moisture content and root development (Kendy et al., 2003; Campbell and Norman, 1998).

$$\tau = exp[(-kb) * LAI] \quad (4)$$

$$E_p = (\tau)(ET_p) and T_p = (1-\tau)(ET_p) \quad (5)$$

Where τ is the dimensionless fraction of incident beam radiation that penetrates the canopy, *kb* is the dimensionless canopy extinction coefficient, with a value of about 0.82 (Stockle, 1985), *LAI* is leaf-area index, daily values of which can be obtained by simulation of EPIC and ET_p is potential evapotranspiration (mm).

Actual ET can be limited by the availability of water in the soil. Input data include the daily leaf area index (LAI) simulated by the EPIC model and simulated soil moisture in the actual root zone (zone 1) by the WIPE model and the water balance method. The calculation of ET is as follows.

$$E_a = E_p\left[1-\left(\frac{mr}{\theta_{wp}}\right)^{-be}\right] and\ T_a = T_p[1-(\frac{mr}{\theta_{wp}})^{-bt}] \quad (6)$$

$$ET = E_a + T_a \quad (7)$$

Where E_a and T_a are the actual evaporation and transpiration (mm), E_p and T_p are the potential evaporation and transpiration (mm), *mr* is the soil moisture of root zone, θ_{wp} is the wilting point moisture of root zone and *bt* = 4 for transpiration and *be* = 0.4 for evaporation.

2.2.2. Division of hydrological response unit (HRU)

Due to the low spatial heterogeneity of meteorological data in the JFZIA with flat topography, the same meteorological data were used for the entire study area. Considering the distributions of branch canals, sub-lateral canals, groundwater depth and soil texture, the study area was divided into 51 HRUs (Wulahe, Q1-Q9; Qinghui, Q10-Q17; Yangjiahe, Q18-Q35; and Huangji, Q36-Q51) (Fig. S1).

Due to the lack of an actual land use data, the wheat, maize, sunflower and uncultivated areas were simulated with proportions of 23%, 38%, 33% and 6%, respectively, for each HRU (Sun, 2014). The irrigation water depth of each HRU was obtained from canal water dividing the control area. The spatial distribution of HRUs is shown in Fig. 1.

The model was run for each HRU with measured groundwater levels from 2009 to 2013. After the simulations, the groundwater upward flux, crop ET, crop yield and WP for each HRU were calculated as weighted averages according to the ratios of wheat, maize, sunflower and uncultivated land. The spatial distribution of hydrological elements during 2009–2013 was analyzed using element conversion in ArcGIS 10. Then the relationships between the water use indicators and the groundwater fluxes or irrigation amount were investigated using result from 2009 to 2013.

2.2.3. Model calibration and validation at regional scale

Measurements of soil moisture content for 18 sites each year, leaf area index for 2 sites each year and yield for 8 sites in 2012 and 2 sites in 2013 over the crop growing period of the study area were used to calibrate and validate the AWPM-SG model at the regional scale (Fig. 1). The 2012 data were used for calibration and 2013 data were used for validation of the model. The model reproduces the soil moisture of root zone (zones 1 and 2), LAI, groundwater upward flux, ET and crop yield using the observed initial soil moisture content and groundwater depth subject to the irrigation schedules and precipitation. Soil hydraulic parameters (residual soil moisture, θ_r; saturated soil moisture, θ_s; field capacity, θ_{fc} ; soil moisture at wilting point, θ_{wp}; soil constant, *C* and *α*; and saturated hydraulic conductivity, *ks*) and crop parameters (maximum leaf area index, LAI_{mx}; extinction coefficient of the canopy, kb; empirical parameters for evaporation and transpiration, be and bt; energy conversion factor, BE; and harvest index, HI) were calibrated (Tables 1 and 2). During the calibration, we set the parameters of model according to the measured data and recommended values, and we analyzed the sensitivity and uncertainty analysis of parameters (Fig. S4 and Table S1) and found the sensitive parameters for soil water, groundwater depth and crop LAI, respectively such as θ_{fc}, LAI_{mx} and so on. Then we adjust the parameters as their sensitivity to make the simulation result of model closer to measured data. At last the

Table 1
Soil hydraulic parameters in the Jiefangzha Irrigation Area.

Soil types	θ_r (cm^3/cm^3)	θ_s (cm^3/cm^3)	θ_{fc} (cm^3/cm^3)	θ_{wp} (cm^3/cm^3)	ρ (g/cm^3)	K_s (cm/d)
Silt	0.034	0.46	0.37	0.095	1.44	6
Silt loam	0.067	0.45	0.33	0.090	1.45	10.8
Loam	0.078	0.43	0.32	0.081	1.45	24.96
Sandy loam	0.065	0.41	0.31	0.081	1.47	106.1
Sand	0.045	0.43	0.30	0.071	1.50	712.8

Note: θ_r is the residual soil moisture (cm^3/cm^3); θ_s is saturated soil moisture (cm^3/cm^3); θ_{fc} is field capacity (cm^3/cm^3); θ_{wp} is the soil moisture at wilting point (cm^3/cm^3); ρ is bulk density (g/cm^3); K_s is saturated hydraulic conductivity (cm/d).

Table 2
Crop parameters of wheat, maize and sunflower for the crop growth part of AWPM-SG model. be, bt are the empirical parameters for evaporation and transpiration.

Parameters	Wheat	Maize	Sunflower
Dimensionless canopy extinction coefficient, kb	0.2	0.8	0.3
be	0.3	0.3	0.3
bt	4	4	4
Minimun temperature for plant growth, T_b (ºC)	2	8	6
Optimal temperature for plant growth, T_o (ºC)	20	25	20
Leaf area index decline rate, *ad*	0.55	0.75	1
Maximum crop height, h_{mx} (cm)	180	250	80
Maximum leaf area index, LAI_{mx}	6.0	5.5	5
Maximum root depth, RD_{mx} (cm)	90	90	90
Plant radiation-use efficiency, BE [(kg*ha^{-1})/(MJ*m^{-2})]	30	40	45
Harvest index, HI	0.25	0.4	0.15
Total potential heat units required for crop maturation, PHU (ºC)	1850	2100	2050
A parameter expressing the sensitivity of harvest index to drought, WYSF	0.2	0.5	0.27

calibrated parameters were used to validate the model using data of 2013. The initial crop parameters for simulating crop growth were used as the default values in the EPIC model for wheat, maize and sunflower. Initial soil moisture content and groundwater depth were specified according to measurements.

For quantifying the model-fitting performance during the calibration and validation processes, the mean relative error (MRE), root mean square error (RMSE), Nash and Sutcliffe model efficiency (NSE) and coefficient of determination (R^2) were calculated. These indicators were defined as follows (Xu et al., 2015):

A *MRE* (mean relative error) close to 0 indicates good model predictions and is calculated as:

$$MRE = \frac{1}{N}\sum_{i=1}^{N}\frac{(P_i - O_i)}{O_i} * 100\% \quad (8)$$

where N is the total number of observations, and P_i and O_i are the ith predicted and observed values respectively (i = 1,2, …, N).

A *RMSE* (root mean square error) value close to 0 indicates good model predictions and is calculated as:

$$RMSE = \sqrt{\frac{\sum_{i=1}^{N}(P_i - O_i)^2}{N}} \quad (9)$$

A *NSE* (Nash and Sutcliffe model efficiency) close to 1 represents a perfect fit, a *NSE* close to 0 represents the predicted values being near to the averaged measurement, and negative *NSE* values indicate that the mean observed value is a better predictor than the simulated value. The *NSE* is calculated as:

$$NSE = 1 - \frac{\sum_{i=1}^{N}(P_i - O_i)^2}{\sum_{i=1}^{N}(O_i - \overline{O})^2} \quad (10)$$

where $\overline{P}$ and $\overline{O}$ are the predicted and observed mean values, respectively.

A R^2 (coefficient of determination) value close to 1 indicates good model predictions.

$$R^2 = \left[\frac{\sum_{i=1}^{N}(O_i - \overline{O})(P_i - \overline{P})}{[\sum_{i=1}^{N}(O_i - \overline{O})^2]^{0.5}[(P_i - \overline{P})^2]^{0.5}}\right]^2 \quad (11)$$

2.3. Water productivity (WP) and irrigation water productivity (IWP)

WP is the ratio of crop yield to crop ET during the crop growing season, which was calculated as:

$$WP = \frac{Y}{ET} \quad (12)$$

where Y is the crop yield (kg/ha), and ET is the total crop ET during the crop growth period (mm).

IWP is defined as the ratio of crop yield to the seasonal application of irrigation water (Salah et al., 2014), calculated as:

$$IWP = \frac{Y}{I} \quad (13)$$

2.4. Coefficient of irrigation effective utilization (C_{ieu})

C_{ieu} is the ratio of the effective irrigation amount to the actual irrigation amount during the crop growing season, and is an important indicator for evaluating water use at the spatial scale. C_{ieu} is calculated as follows:

$$C_{ieu} = \frac{I_e}{I_g} \quad (14)$$

where I_e is the effective irrigation water (mm), which is the irrigation amount used by crop growth; and I_g is the gross irrigation water applied (mm), which is the irrigation water into the field. In this study, the I_e was calculated based on the crop consumption from irrigation water. Rainfall is minimal and its intensity is low in the study area. Then, all the rainfall was considered as the effective rainfall and completely used by crops. The soil water balance components with shallow groundwater are shown in Fig. S2 in the Supplementary material. The effective irrigation (I_e) was calculated using the following equations:

When $F < 0$, $W_f < W_i$,

$$I_e = ET - P_e - (W_i - W_f) \quad (15)$$

When $F < 0$, $W_f > W_i$,

$$I_e = ET - P_e \quad (16)$$

When $F > 0$, $W_f < W_i$,

$$I_e = ET - P_e - F - (W_i - W_f) \quad (17)$$

When $F > 0$, $W_f > W_i$,

$$I_e = ET - P_e - F \quad (18)$$

where F is the net groundwater upward flux being the water capillary rise(G_f) minus water downward flux (D_p) at water table (mm); P_e is effective rainfall (mm), ET is the crop water use during the crop growing season (mm), which is the value of E plus T; and W_i *and* W_f are the soil water content in the root zone at the initial and final times (mm), respectively.

3. Results

3.1. Calibration and validation of the AWPM-SG model at the regional scale

The data in 2012 were used for calibration and data in 2013 for validation of the AWPM-SG model. Calibrated soil and crop parameters for the model are shown in Tables 1 and 2. Performance of the model can be found in Fig. 6. The results showed that the simulated and measured data were distributed evenly on both sides of the 1:1 line with NSE of 0.72, 0.90, 0.7 and 0.69 for soil water content, groundwater depth, crop leaf area index and crop yield, respectively. In Xu's study (2010), the simulated soil water content, groundwater depth and LAI showed agreement with the measured values resulting in NSE of 0.61, 0.81 and 0.99, respectively. In addition, the RMSEs were 25.53 mm, 0.43 m, 0.59 and 1178 kg/ha for soil water content, groundwater depth, crop leaf area index and crop yield, respectively. Therefore, we considered that the simulation results were accurate enough for our regional study.

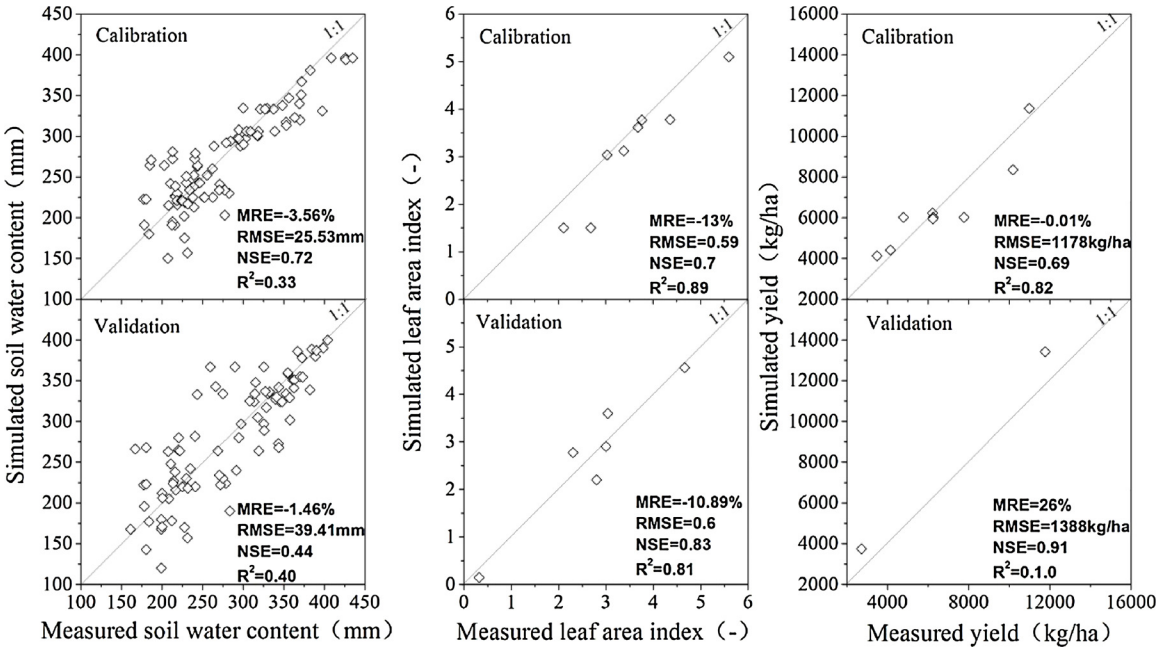

Fig. 6. Comparison of simulated soil and crop indexes with measured soil and crop indexes in 2012 and 2013.

To test the reasonability of the soil parameters and crop parameters, the soil water content, groundwater depth, crop leaf area index and crop yield at 18 sites in 2013 were used for validation (Fig. 6). The results showed that the MRE for soil water content, groundwater depth, crop leaf area index and crop yield ranged from −10.89% to 26%. The R^2 for the four indicators were all greater than 0.4, and NSE were all greater than 0.44. Due to minimal yield data in 2013, the error for crop yield in the validation process was slightly greater.

3.2. Soil water and groundwater changes

The temporal variations of soil water content in the root zone under different groundwater depths during 2009–2013 were analyzed statistically using data of 51 subunits in Fig. 7. The results showed that the averaged soil water content in the root zone decreased as groundwater depth increased due to the low groundwater contribution to soil water in the deep groundwater region. Especially when the groundwater depth was deeper than 2.5 m, the soil water content of the root zone would notably decrease compared with the soil water content under the groundwater depth of 0–2.5 m. Due to low rainfall and deeper groundwater in 2013, the average soil water content was less than that in 2009–2012, especially in areas with deeper groundwater.

Spatially, the average groundwater depth gradually increased from west to east during 2009–2013. During the crop growing season, the average declined value of groundwater levels for five years respectively were 0.42, 0.32, 0.12 and 0.08 m in Wulahe, Yangjiahe, Huangji and Qinghui. Therefore, the groundwater depth decreased less in the regions with deep groundwater, which showed that the groundwater contribution to crop ET in the shallow groundwater regions was much higher than that in the deep groundwater regions.

3.3. Groundwater contribution to ET and effectivity of irrigation water

3.3.1. Groundwater contribution to ET

The spatial distributions of field ET during 2009–2013 are shown in Fig. 8A. ET ranged from 495.61 mm to 787.47 mm over the period of April to September for the five years. At the regional scale, the crop ET values in the central parts of the study area were higher than those in the other parts. In the calculation of this model, groundwater upward flux was related to soil saturated hydraulic conductivity positively, then low soil saturated conductivity lead to less groundwater upward flux and crop ET (Fig. 3) in the western part of the study area. In the eastern part of the study area deep groundwater lead to less capillary rise, which resulted in less crop ET (Fig. 4).

Shallow groundwater contribution to crop growth is important to determine irrigation scheduling. Here, groundwater upward flux was used as the contribution of groundwater to ET. In this study, the groundwater upward flux (F) was the net upward flux at the water table, which is the upward flux minus the downward flux at the water table. The spatial distributions of groundwater upward flux (net groundwater contribution to soil water, F) during 2009–2013 are shown in Fig. 8B. At the regional scale, groundwater upward flux gradually decreased from west to east. The maximum groundwater upward flux was 248.04 mm, 298.23 mm, 300.10 mm, 90.13 mm and 172.74 mm during 2009–2013, respectively. Because of more rainfall in 2012, the groundwater upward flux was less than those in other years. Then, in the Hetao irrigation district with shallow groundwater, the groundwater contribution to crop growth was significant.

Furthermore, groundwater upward flux has a significant seasonal trend from 2009 to 2013 (Fig. 9). In May and June, the groundwater upward flux was negative, meaning the percolation of soil water was greater than groundwater upward flux. This was because in May and June, the crops have enough irrigation water supplied compared to the field crop water use, while in July and August, the crop ET was greater than irrigation, so the groundwater upward flux at this time was much greater than that in the other period. In September, the groundwater upward flux and crop ET began to decrease.

3.3.2. Coefficient of irrigation effective utilization

The spatial distributions of C_{ieu} during 2009–2013 are shown in Fig. 10A and B. In the five years, the greater C_{ieu} was concentrated in the central and eastern parts and lower C_{ieu} was concentrated in the western part (Wulahe area). At Wulahe area, the average C_{ieu} of five years was only about 0.6, which was due to the large irrigation amount in this region. In the northeastern and southeastern parts, the lower C_{ieu} was caused by the deeper groundwater. Then at the deep groundwater district, the percolating water could not be well reused by crops. The C_{ieu} ranged from 0.39–0.93, 0.48–0.95, 0.32–1.0, 0.20–0.98 and 0.39–1.0 for 2009–2013, respectively.

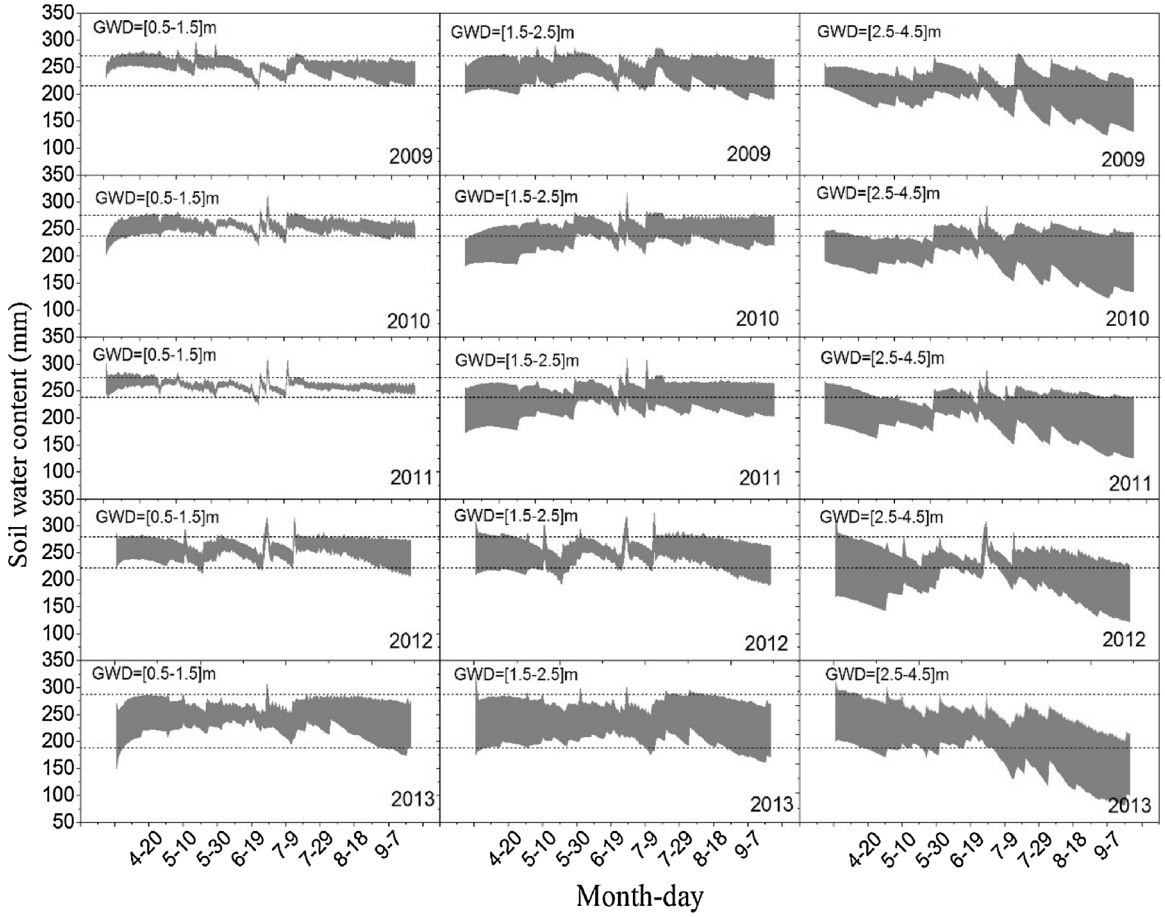

Fig. 7. Temporal variation of soil water content in root zone under different groundwater depth during 2009–2013. GWD—groundwater depth; The two lines were set to contrast the soil moisture under different groundwater depth.

3.4. Spatial distribution of WP and IWP

3.4.1. Relative yield

The relative yield was the ratio of simulated crop yield to the local average crop yield. Since there were different crop species in the study area, the relative yield was used to describe the distributions of crop yield at the regional scale during 2009–2013 (Fig. S3). The relative yield ranged from 0.94 to 1.33, 0.68–1.28, 0.69–1.26, 0.55–1.27 and 0.59–1.31 during 2009–2013 at the regional scale. From the regional distribution, the greater relative yield appeared in the central and eastern regions of the study area, which was consistent with the distribution of crop ET. Then similar to the findings of Gao et al., 2017a,b, the crop yield was proportional to the crop ET.

3.4.2. Water productivity and irrigation water productivity

The spatial distributions of WP during 2009–2013 are shown in Fig. 11A. In the five years, the WP slightly fluctuated from 1.50 kg/m^3 to 2.22 kg/m^3 at the regional scale. Specifically, the WP in the southeastern part was greater than that in other parts of the study area. This could be attributed to the fact that the average groundwater depth of approximately 2.5 m in the southeastern part (Qinghui area) was the appropriate groundwater depth for WP. With the application of water-saving measures, the WP gradually increased with WP values for 2009–2013 of 1.83, 1.79, 1.90, 1.97 and 2.02 kg/m^3, respectively. In agreement with the study of Huo et al. (2012), the WP was mainly affected by irrigation amounts and groundwater depth in this relatively dry region.

Irrigation water productivity (IWP) is the ratio of crop yield to the actual irrigation amount. The spatial distributions of IWP during 2009–2013 in the study area are shown in Fig. 11B. The IWP ranged from 1.04 kg/ m^3 to 8.73 kg/m^3 in the five years. And due to greater rainfall and lower irrigation in 2012, the average IWP of 3.22 kg/m^3 in 2012 was less than the average IWP of 3.27, 3.84, 3.36 and 4.36 kg/m^3 in other four years. Different from the spatial distribution of WP, the IWP in the northeastern part (Yangjiahe and Huangji areas) was greater than that in the other parts. This result was directly related to the distributions of yield and irrigation. Especially in 2012, the irrigation amount in the northeastern part was lower than that in the other parts.

4. Discussion

4.1. Relationship between groundwater upward flux to evapotranspiration (F/ET) and average groundwater depth

To understand the seasonal trend of the impact of groundwater depth on F/ET, the relationship between the monthly groundwater contribution to crop ET (F/ET) and groundwater depth from 2009 to 2013 was analyzed in Fig. 12A. The results indicated that the F/ET decreased from 45% in April to −80% in June and increased from −80% in June to 50% in September of 2012. However, groundwater became shallower from April to June due to the recharge from soil water thawing. A significant trend was found where groundwater depth declined from 1.3 m in June to 1.8 m in September of 2012, and this could be attributed to the groundwater upward flux due to crop evapotranspiration. Although groundwater became deeper and deeper, a higher water requirement of the crops resulted in the groundwater contribution to crop water consumption (F/ET) increasing from June to September. Additionally, crop development stage is an important factor

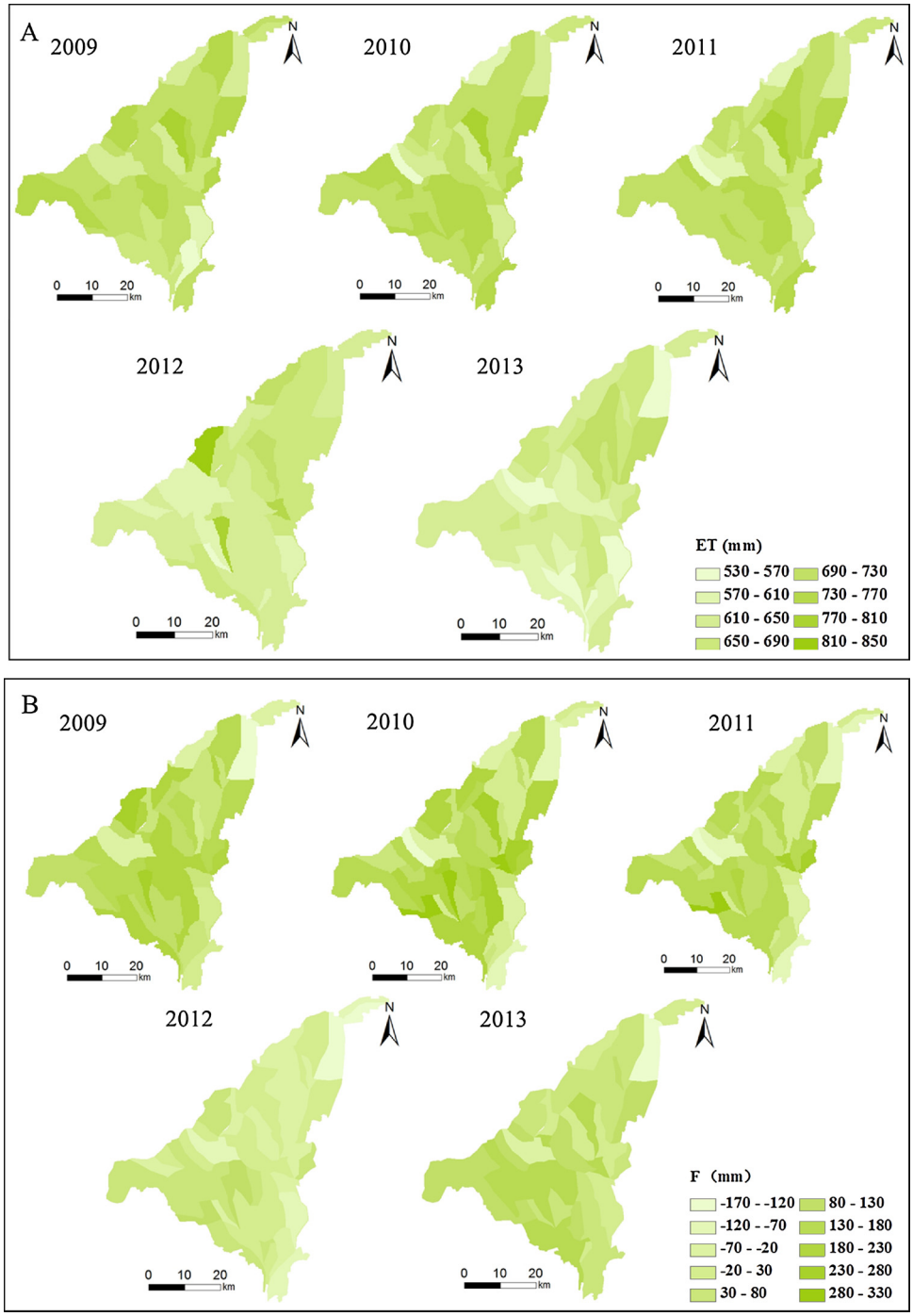

Fig. 8. Spatial distribution of crop evapotranspiration (A) and groundwater upward flux (B) in JFZIA during 2009–2013.

affecting groundwater evaporation (Wang et al., 2016). The high F/ET values of 87%, 97%, 85%, 40% and 75% in April from 2009 to 2013, respectively, were due to the groundwater upward flux under freezing and thawing and high wind speed in spring leading to high evaporation.

The F, ET and F/ET changing with groundwater depth over the crop growing period were statistically analyzed (Fig. 12B). The groundwater upward flux obviously decreased with groundwater depth from groundwater of 1.0 m to 4.5 m at the regional scale. Lower soil water content under deep groundwater confirmed this result. When the groundwater depth was greater than 2.5–3.0 m, the groundwater upward flux varied from positive values to negative values, which showed that the groundwater contributing to crop growth was less than the soil water percolating to groundwater. Exceptionally, when the groundwater depth was between 0.5 m–1.0 m, the groundwater upward flux was less than that with groundwater depth of 1.0 m–1.5 m. This was due to the low soil saturated conductivity and low groundwater evaporation in this area with a groundwater depth of 0.5–1.0 m. Based on experimental and numerical models, previous research has concluded that shallower groundwater can produce greater groundwater upward flux in arid and semi-arid regions (Grismer and Gate, 1988). Based on lysimetric experiments, Ghamarnia et al. (2013) reported that the groundwater contribution decreased from 65% to 38% when groundwater depth decreased from 0.60 m to 1.10 m. Xu et al. (2015) reported that the groundwater contribution to crop growth was significant when the depth of the groundwater table was less than 1.50 m but was irrelevant for depths over 2.00 m.

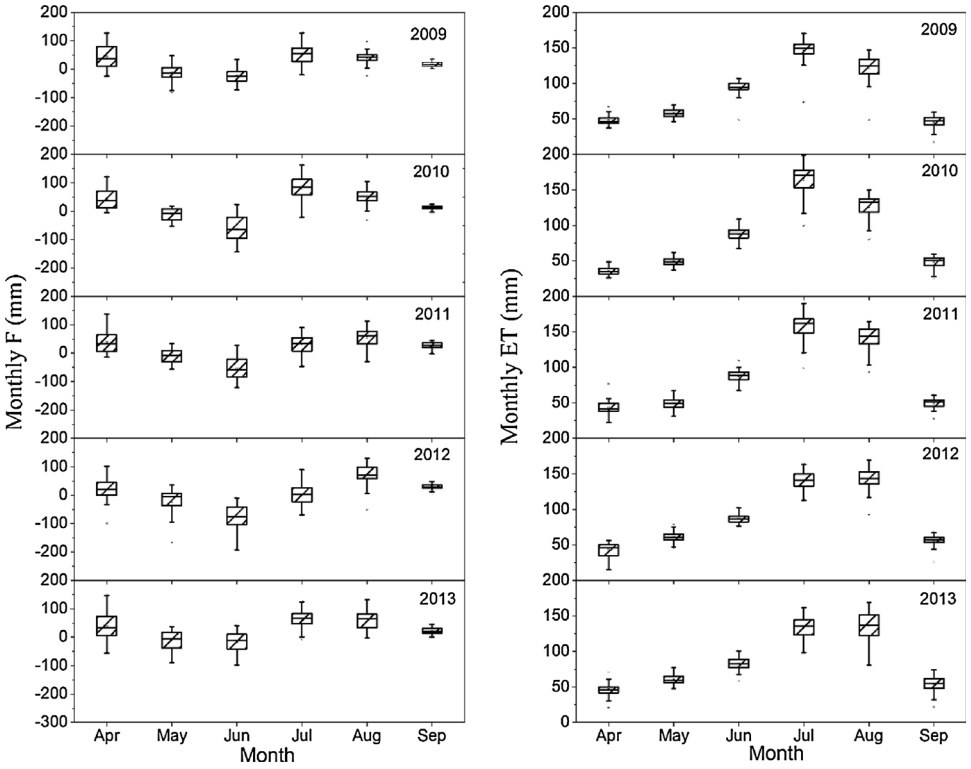

Fig. 9. Temporal variation of monthly F and ET during 2009–2013. F–net groundwater contribution to soil water, which is the capillary rise water minus downward flux at water table (mm); " + " refers to that the groundwater capillary rise to soil water is much than the soil water percolating to groundwater; "-" refers to that the groundwater capillary rise to soil water is less than the soil water percolating to groundwater; ET–crop evapotranspiration (mm).

Compared with the trend of F, the crop ET decreased slightly with deeper groundwater. When the groundwater depth ranged from 1.0 m to 3.0 m, crop ET was approximately 690 mm. However, the average crop ET during the groundwater depths of 0.5–1.0 m were 660 mm, which was attributed to less groundwater upward flux in this region. Similar to the findings of Luo and Sophocleous (2010), ratios of seasonal groundwater evaporation to seasonal potential ET were plotted against the depth to the water table (Fig. 12). When the groundwater was deeper than 3.0 m, the crop ET decreased significantly due to a lack of groundwater upward flux to crop growth under deeper groundwater. This result could be attributed to lower groundwater upward flux to soil leading to low soil water content in the deep groundwater district mentioned in the previous description.

The effect of groundwater depth on the groundwater contribution to crop ET (F/ET) is shown in Fig. 12B. The variation trend was consistent with the tendency of groundwater upward flux at the regional scale. With groundwater depths of 1.0 m to 4.5 m, the F/ET obviously decreased with the decline of groundwater levels. With the groundwater depths of 1.0 m to 1.5 m, the F/ET varied up to 65%. These results are in agreement with the findings of previous studies, and the contribution

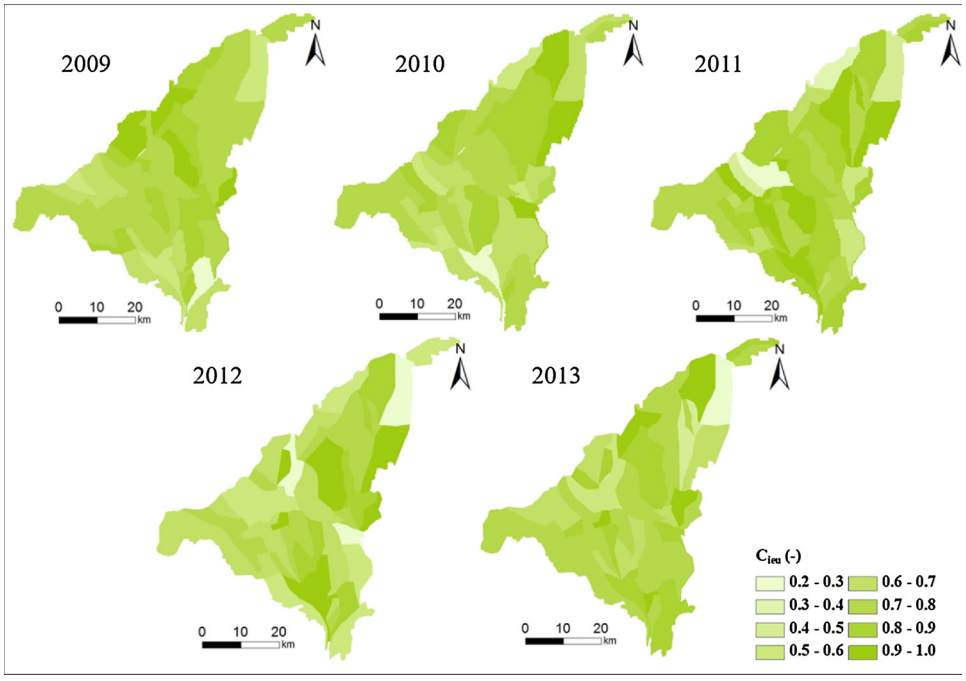

Fig. 10. Spatial distribution and comparison of IWP in JFZIA during 2009–2013. C_{ieu}—Coefficient of irrigation effective utilization.

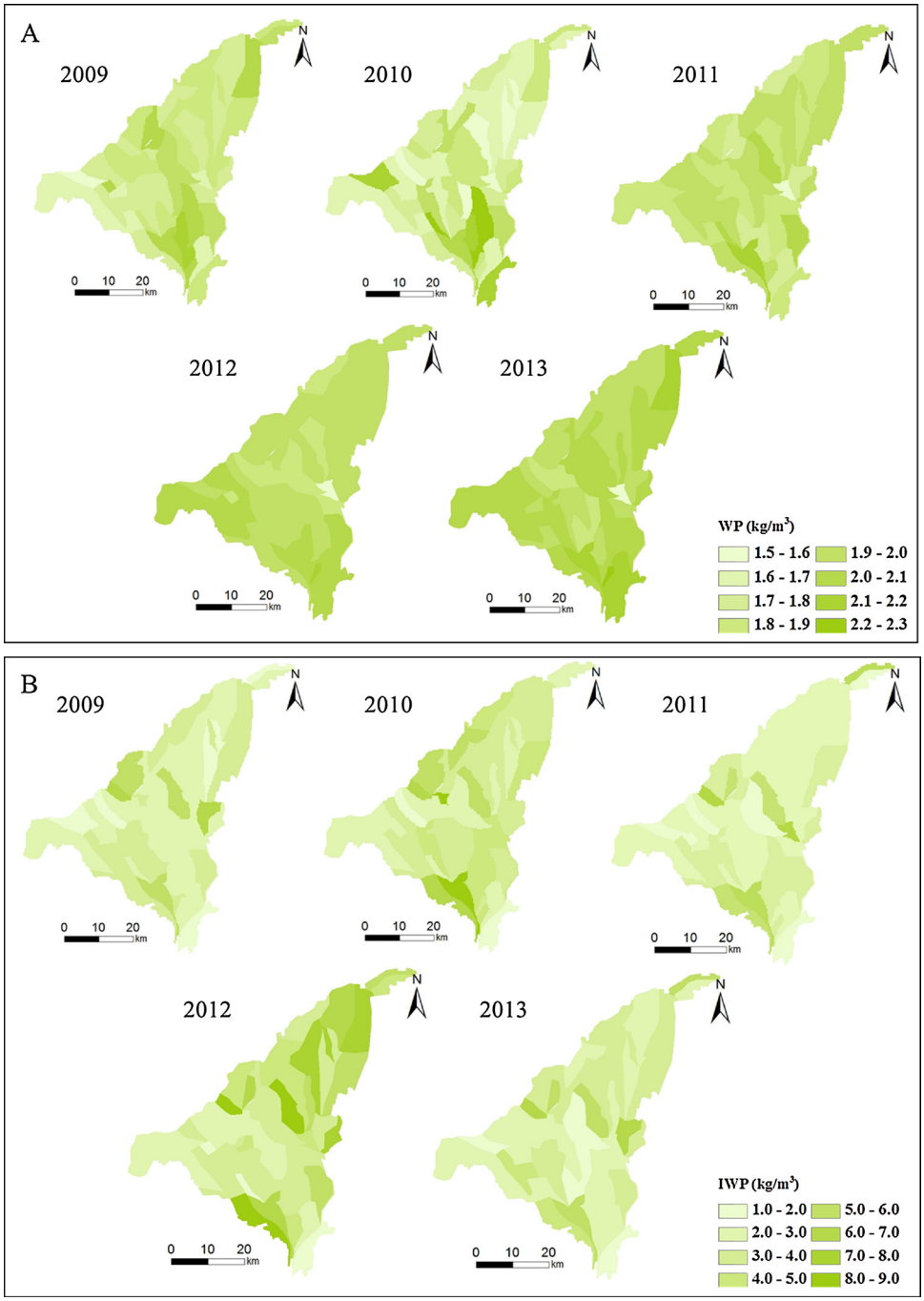

Fig. 11. Spatial distribution of WP (A) and IWP (B) in JFZIA during 2009–2013. WP—Water productivity (kg/m^3), IWP—Irrigation water productivity (kg/m^3).

of groundwater to ET increased with a rising water table and decreased from 90% to 7% when the water table depth increased from 50 cm to 150 cm for the silt clay loam with lysimeters experiments of constant water table depths in the greenhouse (Torres and Hanks, 1989; Kahlown et al., 2005; Karimov et al., 2014). When the groundwater depth is greater than 3.0 m, the groundwater cannot rise through capillary action to the root zone, but some irrigation water can still percolate to the groundwater. Similarly, Luo and Sophocleous (2010) investigated the extinction depth of groundwater evaporation that was approximately 3.8 m. In addition, the effect of the groundwater level on groundwater upward flux is also related to the soil texture, crop growing season and climate condition. Especially, the irrigation can also significantly affect the groundwater upward flux. Furthermore, the groundwater depth can change the efficiency of irrigation water to some extent, which is due to a part of the deep seepage irrigation water being able to be reused.

4.2. Relationship between water productivity and groundwater depth under various irrigation amounts

4.2.1. Relationship between C_{ieu} and groundwater depth

The relationship between C_{ieu} and groundwater depth under various irrigation amounts is shown in Fig. 13A. The C_{ieu} decreased slightly with increasing groundwater depths. This can be attributed to more ET in the shallow groundwater region and deeper groundwater leading to less capillary rise (Yang et al., 2015). In addition, the rate of decline in C_{ieu} would be much smaller when irrigation amounts increased which showed that the effect of groundwater depth on C_{ieu} would be weakened

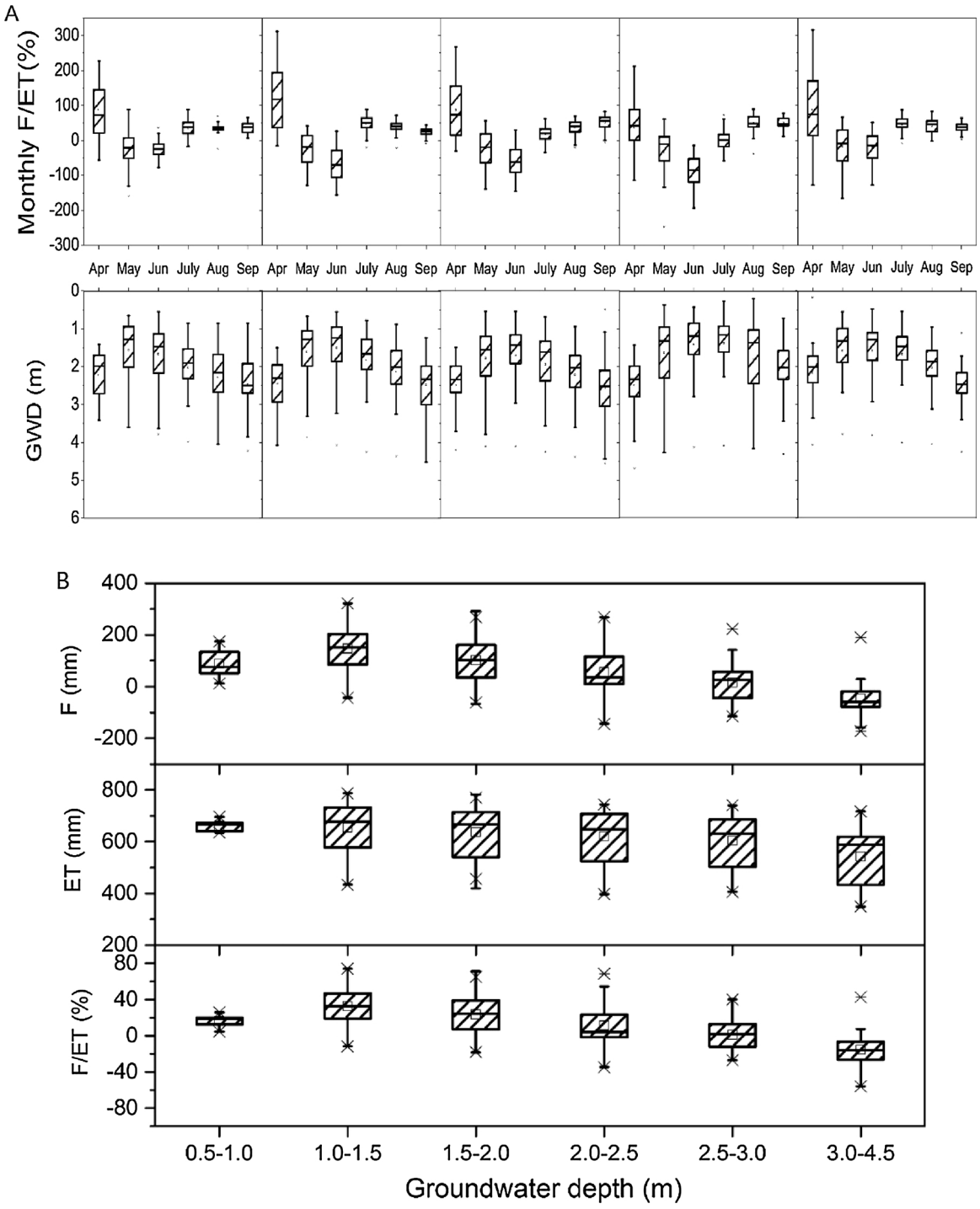

Fig. 12. Relationship between monthly F/ET and groundwater depth (A), seasonal F, ET, F/ET and groundwater depth (B) using 5-year simulation results (2009–2013). "+" refers to the groundwater capillary rise to soil water much than the soil water percolating to groundwater during crop growing season; "-" refers to groundwater capillary rise to soil water less than the soil water percolating to groundwater during crop growing season.

with increased irrigation. This could be attributed to the fact that the groundwater contributions would decrease with increasing irrigation amounts (Gao et al., 2017a,b). The rate of decline in C_{ieu} was 0.07, 0.06, 0.04 and 0.03 with irrigation amounts of 100–300 mm, 300–400 mm, 400–500 mm and 500–900 mm, respectively. Overall, the C_{ieu} focused on 0.6 to 1.0.

4.2.2. Relationship between water productivity (WP) and groundwater depth

Influenced by crops, soil conditions, groundwater depth and agricultural practices including fertilization and atmospheric factors, WP varies both spatially and temporarily (Hatfield et al., 2001; Cox et al., 2002). Based on the statistical analysis of data for 51 HRUs from 2009 to 2013, the WP under various groundwater depths and irrigation amounts at the regional scale is shown in Table 3. Though there was little difference of WP at the regional scale, the mean WP was related to the distribution of groundwater depth with a slightly parabolic trend. Overall, when the groundwater depth was less than 3.0 m, the WP increased with increasing groundwater depth, and then the WP began to decrease with groundwater depths greater than 3.0 m. The average WP

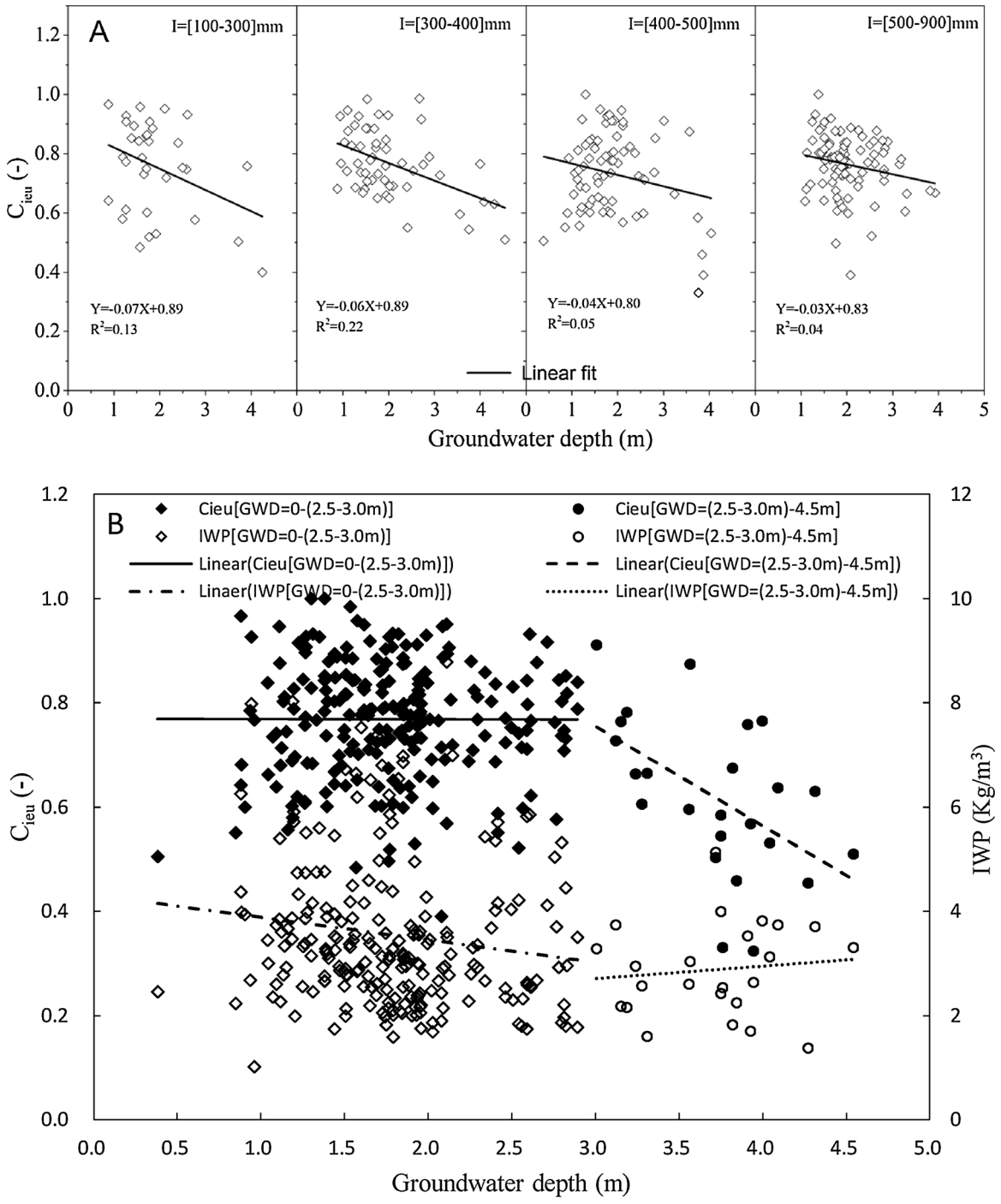

Fig. 13. (A) Relationship between C_{ieu} and groundwater depth under various irrigation amount using 5-year simulation results (2009–2013). C_{ieu}—Coefficient of irrigation effective utilization; I—irrigation amount (mm); The two lines were set to compare the slope of the trend lines. (B) Relationship between C_{ieu}, IWP and groundwater depth using 5-year simulation results (2009–2013). IWP — Irrigation water productivity; GWD —Groundwater depth.

Table 3
Water productivity under various groundwater depths and irrigation amount (kg/m^3).

Irrigation Amount(mm)	Groundwater depth (m)						
	0.5-1.0	1.0-1.5	1.5-2.0	2.0-2.5	2.5-3.0	3.0-4.5	Mean
100-300	1.87(±0.04)	1.92(±0.12)	1.93(±0.16)	1.92(±0.19)	2.02(±0.11)	1.98(±0.04)	1.94(±0.05)
300-500	1.86(±0.13)	1.89(±0.14)	1.90(±0.14)	1.91(±0.15)	1.87(±0.16)	1.90(±0.10)	1.89(±0.02)
500-700		1.77(±0.18)	1.89(±0.18)	1.89(±0.14)	1.87(±0.12)	1.83(±0.18)	1.87(±0.02)
700-900			1.86(±0.13)	1.87(±0.14)	1.87(±0.10)		1.87(±0.01)
Mean	1.87(±0.01)	1.89(±0.03)	1.90(±0.03)	1.90(±0.02)	1.91(±0.07)	1.90(±0.07)	

Table 4
Irrigation water productivity under various groundwater depths and irrigation amounts (kg/m^3).

Irrigation Amount(mm)	Groundwater depth (m)						
	0.5-1.0	1.0-1.5	1.5-2.0	2.0-2.5	2.5-3.0	3.0-4.5	Mean
100-300	5.81(±1.32)	5.80(±1.03)	6.08(±1.26)	6.21(±1.62)	5.13(±1.23)	4.42(± 0.81)	5.83(±0.67)
300-500	3.76(±1.90)	3.70(±0.90)	3.95(±1.41)	3.61(±0.82)	3.52(±1.07)	3.16(± 0.55)	3.62(±0.26)
500-700		2.63(±0.39)	2.64(±0.52)	2.92(±0.90)	2.52(±0.34)	1.97(±0.41)	2.54(±0.34)
700-900			1.77(±0.40)	1.82(±0.11)	1.72(±0.11)		1.77(±0.05)
Mean	4.79(±1.40)	4.04(±1.58)	3.61(±1.87)	3.64(±1.8)6	3.22(±1.46)	3.18(±1.22)	

at 0.5–1.0 m, 2.5–3.0 m and 3.0–4.5 m during 2009–2013 were 1.87, 1.91 and 1.90 kg/m^3, respectively, which illustrated that invalid groundwater evaporation that groundwater upward flux unused by crop growing existed under shallower groundwater and water stress affected crop transpiration under deeper groundwater with lower soil water content. On the other hand, with irrigation water increasing, the WP decreased gradually. Thus, simulations seem to agree with the earlier findings of Huo et al. (2012) and Gao et al., 2017a,b, where with appropriate irrigation, the relationship between WP and groundwater depth had a parabolic trend. In agreement with Mueller et al. (2005), the water use efficiency (WUE) of wheat could be enhanced with deeper groundwater tables to some extent.

4.2.3. Relationship between irrigation water productivity (IWP) and groundwater depth

Irrigation water productivity (IWP) is affected by groundwater depth, irrigation amount, soil texture and climate. The IWP under various groundwater depths and irrigation amounts at the regional scale from 2009 to 2013 is shown in Table 4. The results showed that the IWP decreased with increasing irrigation amounts for each groundwater depth. The mean IWP decreased from 5.83 to 1.77 kg/m^3, while the irrigation amount increased from 100 to 900 mm. In agreement with the findings of Howell et al. (1997) and Huang et al. (2005), the irrigation water-use efficiency for biomass and grain yield decreased with increasing irrigation. On the other hand, the effect of groundwater depth on IWP was generally linear. The IWP decreased with the decline of the groundwater table under the same irrigation application, which was due to more groundwater upward flux to crop growing in the shallow groundwater district and less groundwater upward flux with deep groundwater. Similar to the previous study of Huo et al. (2012), the IWP significantly decreased with the decline of the groundwater table under the same irrigation water application, attributable to the shallow groundwater contributing to crop water use.

Comparing the impact of groundwater depth on IWP and C_{ieu}, the relationship between IWP and C_{ieu} was proportionally linear under groundwater depths of 0 to 2.5–3.0 m, while the descending rate of C_{ieu} increased and the IWP varied gently under groundwater depths of 2.5–3.0 m to 4.5 m (Fig. 13B). This could be attributed to low groundwater upward flux and more irrigation percolation under deep groundwater. Furthermore, the deep groundwater could not provide more water to crop growing and then IWP would be affected insignificantly. Therefore, according to the irrigation schedule and crop growing, the optimal groundwater depth was 2.5–3.0 m in this study area.

5. Conclusions

Based on the AWPM-SG model, the spatial distributions of groundwater upward flux, crop ET, crop yield and WP in the Jiefangzha Irrigation area from 2009 to 2013 were simulated. Furthermore, the regional groundwater contribution to crop water use and efficiency of irrigation water were quantified from the regional simulation results. The groundwater contribution to ET and C_{ieu} are higher in fields with shallower groundwater of 1.0–3.0 m and the F/ET would be up to 65% during the groundwater depth of 1.0–1.5 m.

Groundwater contributions to ET can greatly increase biomass productivity. The maximum WP appeared in the district with groundwater depths of approximately 3.0 m. Meanwhile, the distributions of IWP were correlated with the distribution of groundwater depth. From the relationship between IWP and C_{ieu} under various groundwater levels, the optimal groundwater depth under the circumstances for these irrigated crops was 2.5 m – 3.0 m in the study area. Overall, for enhancing the efficiency of irrigation water and irrigation water productivity, irrigation schedule need to be optimized by considering groundwater contributions to ET in shallow groundwater field in arid and semi-arid areas. Furthermore, the contribution varies with other factors, including soil texture and climate condition. In future studies, researchers should further investigate the impact of multiple factors on shallow groundwater contributions to agricultural WP.

Acknowledgements

This research was supported by National Natural Science Fundation of China (51639009, 51679236) and National Key Research and Development Program of China (2017YFC0403301). The contributions of the editor and anonymous reviewers whose comments and suggestions significantly improved this article are also appreciated.

Appendix A. Supplementary data

Supplementary material related to this article can be found, in the online version, at doi:https://doi.org/10.1016/j.agwat.2018.06.009.

References

Allen, R., Pereira, L., Raes, D., Smith, M., 2006. Crop Evapotranspiration. FAO Irrigation and Drainage Paper No. 56.
Bouman, B., 2007. A conceptual framework for the improvement of crop water productivity at different spatial scales. Agric. Syst. 93, 43–60.
Brunner, P., Li, H.T., Kinzelbach, W., Li, W.P., Dong, X.G., 2008. Extracting phreatic evaporation from remotely sensed maps of evapotranspiration. Water Resour. Res. 44, W08428.
Cai, L.G., Mao, Z., Fang, S.X., Liu, H.S., 2003. The yellow River basin and case study areas. In: Pereira, L.S., Cai, L.G., Musy, A., Minhas, P.S. (Eds.), Water Saving in the Yellow River Basin: Issue and Decision Support Tools in Irrigation. China Agricultural Press, Beijing, pp. 13–34.
Campbell, G.S., Norman, J.M., 1998. An Introduction to Environmental Biophysics, 2nd edition. Springer-Verlag, New York, pp. 249.
Cox, J.W., McVicar, T.R., Reuter, D.J., Wang, H., Cape, J., Fitzpatrick, R.W., 2002. Assessing rainfed and irrigated farm performance using measures of water use efficiency. In: McVicar, T.R., Rui, L., Walker, J., Fitzpatrick, R.W., Chanming, L. (Eds.), Regional Water and Soil Assessment for Managing Sustainable Agriculture in China and Australia. Australian Centre for International Agricultural Research, Canberra, Australia, pp. 70–81.
Cynthia, R., Joshua, E., Delphine, D., et al., 2014. Assessing agricultural risks of climate change in the 21st century in a global gridded crop model intercomparison. Proc. Natl. Acad. Sci. U. S. A. 111, 3268–3273.
Dalin, C., Qiu, H., Hanasaki, N., 2015. Balancing water resources conservation and food security in China. Proc. Natl. Acad. Sci. U. S. A. 112, 4588–4593.
De Wit, C.T., Brouwer, R., Penning de Vries, F.W.T., 1970. The simulation of photosynthetic systems. In: Setlik, I. (Ed.), In Prediction and Management of Photosynthetic Productivity, Proceedings of the International Biological Program/Plant Production Technical Meeting, Trebon. PUDOC, Wageningen, The Netherlands, pp. 47–70.
Diepen, C.A., Wolf, J., van Keulen, H., Rappoldt, C., 1989. WOFOST: a simulation model

of crop production. Soil Use Manage. 5 (1), 16–24.
Gao, X.Y., Bai, Y.N., Huo, Z.L., Huang, G.H., Xia, Y.H., Steenhuis, S.T., 2017a. Deficit irrigation enhances contribution of shallow groundwater to crop water consumption in arid area. Agric. Water Manage. 185 (2017), 116–125.
Gao, X.Y., Huo, Z.L., Qu, Z.Y., Xu, X., Huang, G.H., Steenhuis, S.T., 2017b. Modeling contribution of shallow groundwater to evapotranspiration and yield of maize in an arid irrigation district using readily available data. Sci. Rep., srep43122.
Gardner, W.R., 1958. Some steady-state solutions of the unsaturated moisture flow equation with application to evaporation from a water table. Soil Sci. 85, 228–232.
Ghamarnia, H., Golamian, M., Sepehri, S., Arji, I., Norozpour, S., 2013. The contribution of shallow groundwater by safflower (*Carthamus tinctorius L.*) under high water table conditions, with and without supplementary irrigation. Irrig. Sci. 31, 285–299.
Grismer, M.E., Gate, T.K., 1988. Estimating saline water table contribution to crop water use. Calif. Agric. 42 (2), 23–24.
Hanson, J., Ahuja, L., Shaffer, M., Rojas, K.W., DeCoursey, D.G., Farahani, H., Johnson, K., 1998. RZWQM: simulating the effects of management on water quality and crop production. Agric. Syst. 57 (2), 161–195.
Hatfield, J.L., Sauer, T.J., Prueger, J.H., 2001. Managing soils to achieve greater water use efficiency: a review. Agron. J. 93 (March/April (2)), 271–280.
Herzog, L.B., Larson, D.R., Abert, C.C., Wilson, D.S., Roadcap, S.G., 2003. Hydrostratigraphic modelling of a complex, glacial-drift aquifer system for importation into MODFLOW. Ground Water 41 (1), 57–65.
Howell, T.A., Schneider, A.D., Evett, S.R., 1997. Subsurface and surface microirrigation of corn-Southern high plains. Trans. ASAE 40, 635–641.
Huang, Y.L., Chen, L.D., Fu, B.J., Gong, J., 2005. The wheat yields and water-use efficiency in the loess plateau: straw mulch and irrigation effects. Agric. Water Manage. 72 (3), 209–222.
Huo, Z.L., Feng, S.Y., Huang, G.H., Zheng, Y.Y., Wang, Y.H., Guo, P., 2012. Effect of groundwater level depth and irrigation amount on water fluxes at the groundwater table and water use of wheat. Irrig. Drain. 61, 348–356.
Jaksa, W., Sridhar, V., 2015. Effect of irrigation in simulating long-term evapotranspiration climatology in a human-dominated river basin system. Agric. For. Meteorol. 200, 109–118.
Jha, M., Chowdhury, A., Chowdary, V., Peiffer, S., 2007. Groundwater management and development by integrated remote sensing and geographic information systems:prospects and constraints. Water Resour. Manage. 21 (2), 427–467.
Jones, J., Hoogenboom, G., Porter, C., et al., 2003. The DSSAT cropping system model. Eur. J. Agron. 18, 235–265.
Kahlown, M.A., Ashraf, M., Zia-ul-Haq, 2005. Effect of shallow groundwater table on crop water requirement and crop yields. Agric. Water Manage. 76, 24–35.
Karimov, A.H., Simunek, J., Hanjra, M.A., Avliyakulov, M.M., Forkutsa, I., 2014. Effects of the shallow water table on water use of winter wheat and ecosystem health: implications for unlocking the potential of groundwater in the Fergana Valley (Central Asia). Agric. Water Manage. 131, 57–69.
Kendy, E., Gerard-marchant, P., Todd Walter, M., Zhang, Y.Q., Liu, C.M., Steenhuis, S.T., 2003. A soil-water –balance approach to quantify groundwater recharge from irrigated cropland in the North China Plain. Hydrol. Process. 17 (10), 2011–2031.
Li, H.S., Wang, W.F., Zhang, G.B., Zhang, Z.M., Wang, X.W., 2011. GSPAC water movement in extremely dry area. J. Arid Land 3 (2), 141–149.
Liu, Z.Y., Chen, H., Huo, Z.L., Wang, F.X., Shock, C.C., 2016. Analysis of the contribution of groundwater to evapotranspiration in an arid irrigation district with shallow water table. Agric. Water Manage. 171, 131–141.
Luo, Y., Sophocleous, M., 2010. Seasonal groundwater contribution to crop-water use assessed with lysimeter observations and model simulation. J. Hydrol. 389 (3), 325–335.
Morison, J., Baker, N., Mullineaux, P., Davies, W.J., 2008. Improving water use in crop production. Philos. Trans. R. Soc. B 363, 639–658.
Mueller, L., Behrendt, A., Schalitz, G., Schindler, U., 2005. Above ground biomass and water use efficiency of crops at shallow groundwater tables in a temperate climate. Agric. Water Manage. 75 (2), 117–136.
Nishida, K., Shiozawa, S., 2010. Modeling and experimental determination of salt accumulation induced by root water uptake. Soil Sci. Soc. Am. J. 74, 774–786.
Ragab, R.A., Fathi, Amer, 1986. Estimating water table contribution to the water supply of maize. Agric. Water Manage. 11, 221–230.
Ritchie, J.T., 1972. Model for predicting evaporation from a row crop with incomplete cover. Water Resour. Res. 8, 1204–1213.
Salah, E.E., Maher, A.K., Nasser, A.A., Urs, S., 2014. Optimal coupling combination between the irrigation rate and glycine betaine levels for improving yield and water use efficiency of drip-irrigated maize grown under arid conditions. Agric. Water Manage. 140, 69–78.
Saleh, A., Steenhuis, T., Walter, M., 1989. Groundwater table simulation under different rice irrigation practices. J. Irrig. Drain. E 115 (4), 530–544.
Santoni, C.S., Jobbagy, E.G., Contreras, S., 2010. Vadose zone transport in dry forests of central Argentina: role of land use. Water Resour. Res. 46, W10541.
Sau, F., Boote, K.J., Bostick, W.M., et al., 2004. Testing and improving evapotranspiration and soil water balance of the DSSAT crop models. Agron. J. 96, 1243–1257.
Schoups, G., Hopmans, J., Young, C., Vrugt, J.A., Wallender, W.W., Tanji, K.K., Panday, S., 2005. Sustainability of irrigated agriculture in the San Joaquin vally, California. Proc. Natl. Acad. Sci. U. S. A. 102, 15352–15356.
Simunek, J., Van Genuchten, M., Sejia, M., 2005. The HYDRUS-1D Software Package for Simulating the One-Dimensional Movement of Water, Heat and Multiple Solutes in Variability-Saturated media. Development of Environment Sciences. University of Califonia, Riverside, California.
Soppe, R.W.O., Ayars, J.E., 2003. Characterizing groundwater use by safflower using lysimeters. Agric. Water Manage. 60, 59–71.
Steenhuis, T.S., Van Der Molen, W.H., 1985. The Thornthwaite-mather procedure as a simple engineering method to predict recharge. J. Hydrol. 84, 221–229.
Stockle, C.O., 1985. Simulation of the effect of water and nitrogen stress on growth and yield of spring wheat. PhD Dissertation. Washington State University, Pullman, WA.
Sun, 2014. The analysis of different scales diversity law of irrigation water efficiency and water saving potential in hetao irrigation area of inner Mongolia. inner Mongolia agricultural university. Hohhot.Torres, J.S., Hanks, R.J., 1989. Modeling water table contribution to crop evapotranspiration. Irrig. Sci. 10 (4), 265–279.
Torres, J.S., Hanks, R.J., 1989. Modeling water table contribution to crop evapotranspiration. Irrig. Sci. 10 (4), 265–279.
Van Dam Jos, C., Groenendijk, P., Hendriks, R.F.A., Kroes, J.G., 2008. Advances of modeling water flow in variably saturated soils with SWAP. Vadose Zone J. 7, 640–653.
Vanuytrecht, E., Raes, D., Hsiao, T.C., Mejias, P., 2014. AquaCrop: FAO's crop water productivity and yield response model. Environ. Modell. Softw. 62, 351–360.
Wang, X.S., Yue, W.F., Yang, J.Z., 2004. Analysis on water cycling in GSPAC system of Tetao-irigation district, in inner Mongolia, China. J. Irrig. Drain. 23 (2), 30–33.
Wang, X.W., Huo, Z.L., Feng, S.Y., Guo, P., Guan, H.D., 2016. Estimating groundwater evapotranspiration from irrigated cropland incorporating root zone soil texture and moisture dynamics. J. Hydrol. 543, 501–509.
Williams, J.R., 1995. The EPIC model. In: Singh, V.P. (Ed.), Computer Models of Watershed Hydrology. 909-1000. Water Resources Publications, Highland Ranch, Colo.
Williams, J.R., Jones, C.A., Kiniry, J.R., Spanel, D.A., 1989. The EPIC crop growth model. Trans. ASAE 32, 497–511.
Wit, K.E., 1967. Apparatus for measuring hydraulic conductivity of undisturbed soil samples. Bull. Inst. Land Water Manage. Res.(52) Wegeningen.
Xu, X., Huang, G.H., Qu, Z.Y., Pereira, L.S., 2010. Assessing the groundwater dynamics and impacts of water saving in the Hetao irrigation District, yellow River basin. Agric. Water Manage. 98, 301–313.
Xu, X., Sun, C., Qu, Z.Y., Huang, W.Z., Ramos, T.B., Huang, G.H., 2015. Groundwater recharge and capillary rise in irrigated areas of the upper yellow River basin assed by an agro-hydrological model. Irrig. Drain. 64, 587–599.
Xue, J.Y., Guan, H.D., Huo, Z.L., Wang, F.X., Huang, G.H., Boll, J., 2017. Water saving practices enhance regional efficiency of water consumption and water productivity in an arid agricultural area with shallow groundwater. Agric. Water Manage. 194, 78–89.
Yang, J., Wan, S., Deng, W., Zhang, G., 2007. Water fluxes at a fluctuating groundwater table and groundwater contributions to wheat water use in the lower yellow River flood plain, China. Hydrol. Process. 21, 717–724.
Yang, X.L., Chen, Y.Q., Pacenka, S., Gao, W.S., Zhang, M., Sui, P., Steenhuis, T.S., 2015. Recharge and groundwater use in the north China Plain for six irrigated crops for an eleven-year period. PLoS One 10 (1), e0115269.
Zhou, A.G., Ma, R., Zhang, C., 2005. Vertical water cycle and its ecological effect in inland basins, Nowthwest China. Adv. Water Sci. 16 (1), 127–133.